Reaction Pathways of the Electron Transfer from Photoexcited 10-Methylphenothiazines to Electron Acceptors in Polar Solvents. Effects of Magnetic Fields and Heavy Atoms on Efficiency of Free Ion Formation

Eriko Shimada,[†] Masae Nagano,[§] Makio Iwahashi,[§] Yukie Mori,*[,‡] Yoshio Sakaguchi,[‡] and Hisaharu Hayashi[‡]

Department of Applied Chemistry, Faculty of Engineering, Kanagawa Institute of Technology, Shimo-ogino, Atsugi, Kanagawa 243-0292, Japan, Department of Chemistry, Faculty of Science, Kitasato University, Kitasato, Sagamihara, Kanagawa 228-8555, Japan, and Molecular Photochemistry Laboratory, RIKEN (The Institute of Physical and Chemical Research), Hirosawa, Wako, Saitama 351-0198, Japan

Received: September 16, 2000; In Final Form: January 4, 2001

The lowest triplet excited states of (2-substituted) 10-methylphenothiazine were found to be quenched by various electron acceptors in polar solvents such as 2-propanol and acetonitrile through electron transfer (ET). The transient absorption and time-resolved EPR spectra indicated that the radical cation of the phenothiazine and radical anions of the acceptors were formed as the ET products in moderate to high yields. These free radical ions were formed via two types of intermediates, (i) a triplet contact radical ion pair (^{3}CRIP) or a triplet exciplex (^{3}Ex*) and (ii) a triplet solvent-separated radical ion pair (^{3}SSRIP). In the quenching by the Br-substituted acceptors, a large fraction of ^{3}CRIP (or ^{3}Ex*) was deactivated to the singlet ground states due to the breakdown of the spin-forbiddance by strong spin−orbit coupling. On the other hand, ^{3}CRIP (or ^{3}Ex*) containing no heavy atom was mainly transformed into ^{3}SSRIP by solvation. ^{3}SSRIP decayed through either the separation to free ions or the triplet−singlet conversion followed by the spin-allowed backward ET to the ground states. The backward ET rates of ^{1}SSRIPs were estimated to be $\geq 10^9$ s^{-1}, even when the reaction fell into the deeply inverted region. In 2-propanol, the free ion yields were affected by magnetic fields. The magnitudes of magnetically induced changes strongly depended on the polarity and viscosity of solvents, suggesting that the separation rate of SSRIP should be a crucial factor determining the field dependence of the free ion yields.

1. Introduction

Electron transfer (ET) is an elementary reaction of great importance in chemistry as well as biochemistry.[1] Especially, photoinduced ET is one of the most active fields in ET chemistry. Since the end of 1980s, mechanisms of photoinduced intermolecular ET between aromatic donors and acceptors in solution have been unraveled by means of picosecond transient absorption and emission spectroscopy.[2−9] Two kinds of radical ion pairs (RIPs) with different distances between the charged centers were characterized as the intermediates of these reactions, and their decay dynamics were elucidated. A simplified description of the reaction pathways from singlet precursors is shown in Scheme 1A. On encounter of the lowest singlet excited (S_1) state of a donor (^{1}D*) and an acceptor (A) in the ground (S_0) state, an electron is transferred from ^{1}D* to A to give a contact radical ion pair (^{1}CRIP) (process A). In polar solvents, ^{1}CRIP is transformed into a solvent-separated radical ion pair (^{1}SSRIP) (process B), where $D^{\bullet+}$ and $A^{\bullet-}$ are separated from each other by intervening solvent molecules. Further separation of $D^{\bullet+}$ and $A^{\bullet-}$ to the bulk of solution gives free ions (process G). In competition with the free ion formation, backward ET within ^{1}CRIP (process C) and/or ^{1}SSRIP (process F) regenerates the S_0 states of D and A. Depending on properties of reactants as well as solvents, several variations of this scheme are available. In some cases partial charge-transfer, instead of full ET, may take place to give an exciplex (^{1}Ex*), which has a mixed character of the localized excited state and the RIP state. ^{1}Ex* decays through several processes such as complete charge separation,[10] deactivation to the S_0 states, and chemical reactions other than ET. In other cases, long-distance ET may directly generate ^{1}SSRIP without intermediacy of ^{1}CRIP (process D).

As for ET reactions involving excited triplet states of chromophores, quite similar reaction pathways can be postulated, as shown in Scheme 1B. A distinctive feature of ET from triplet precursors is that the charge recombination processes from triplet intermediates (^{3}Ex*, ^{3}CRIP, and ^{3}SSRIP) to give the S_0 states are spin-forbidden. Only when strong spin−orbit coupling (SOC) exists are these deactivation channels practically opened (process c). Because of such spin selectivity, the free ion yields and the decay kinetics of the intermediates may be quite different from those for reactions originated from singlet precursors. So far, reduction of the T_1 states of benzophenones[11] and quinones[12−14] through ET or partial charge-transfer from amines and aromatic donors has been studied by many researchers, and formation of radical ion pairs has been observed in polar solvents. However, this type of reaction is sometimes complicated due to competing hydrogen atom transfer, proton-transfer coupled with ET, and subsequent proton transfer within radical ion pairs. Studies on ET reactions with other triplet precursors are rather limited.[15−17] Recently, Sakaguchi and Hayashi reported that 10-methylphenothiazine (MPTZ) in the T_1 state

[†] Kanagawa Institute of Technology.
[§] Kitasato University.
[‡] RIKEN.

10.1021/jp003322y CCC: $20.00
Published on Web 02/23/2001

SCHEME 1: Reaction Pathways in ET Reactions of Excited Donor (D*) with an Acceptor (A)[a]

(A) Singlet Precursor

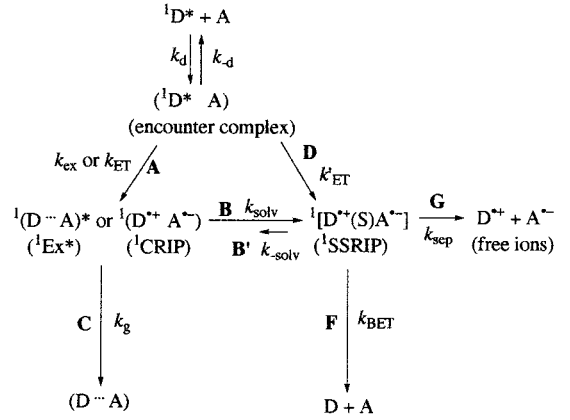

(B) Triplet Precursor

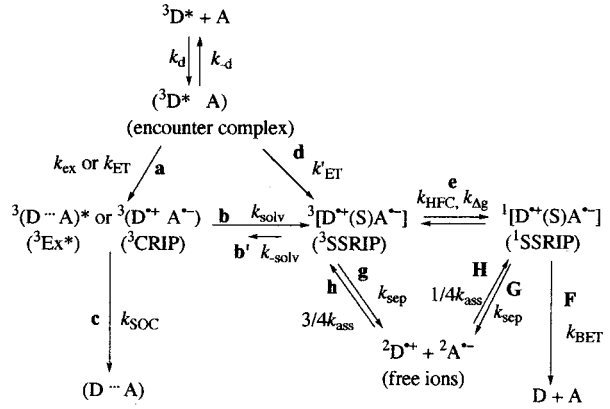

[a] Arrows indicate A and a, ET at a contact distance; B and b, solvation; B′ and b′, collapse to CRIP; C and c, deactivation of Ex* or backward ET of CRIP; D and d, long-distance ET; e, T−S conversion; F, backward ET of ^{1}SSRIP; G and g, separation to free ions; H and h, association of free ions.

donates an electron to 1,4-dicyanobenzene (*p*-DCNB) in 2-propanol (2-PrOH).[18] They investigated magnetic field effects (MFEs) on the yields of free radical ions and showed that the spin conversion of radical ion pair [$MPTZ^{\bullet+}$ p-$DCNB^{\bullet-}$] was affected by magnetic fields. Their results on the MFEs suggest that the precursor of the free ions should be SSRIP, but detailed pathways to give SSRIP are not elucidated.

The aims of this study are (i) to verify the applicability of Scheme 1B to the ET reactions from ^{3}MPTZ* to acceptors such as *p*-DCNB in polar solvents, (ii) to estimate the rate constant of each process in 2-PrOH, which is a solvent often used in studies on MFEs,[19] and (iii) to clarify similarities and differences in mechanisms and kinetics between intermolecular ET reactions with singlet and triplet precursors (Scheme 1A vs 1B). For this purpose, we have studied the photoinduced ET reactions of (2-substituted) 10-methylphenothiazines, (2-X)MPTZ, with various electron acceptors shown in Chart 1 by nanosecond transient absorption spectroscopy. These donors and acceptors were selected so that a wide range of free energy changes were covered without a large difference in molecular size or shape. Effects of magnetic fields on free ion yields, free energy changes accompanying forward and backward ET, heavy atoms, and solvents have been examined. The experimental results have

CHART 1

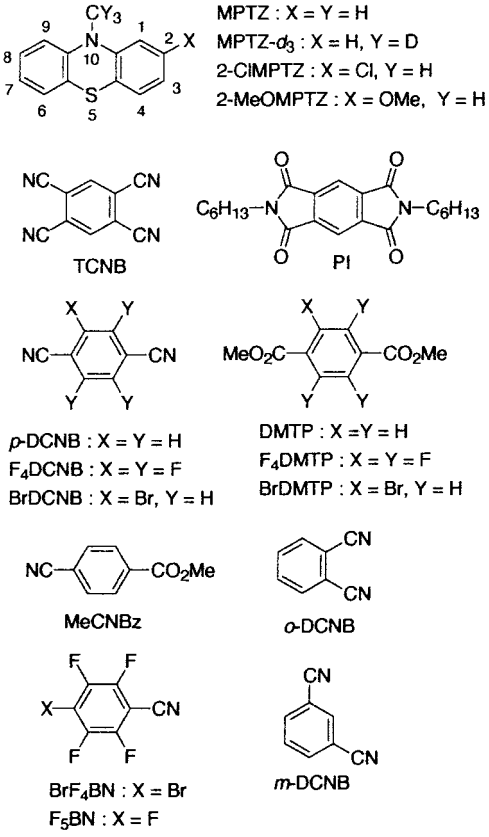

indicated that both CRIP and SSRIP should be formed, which is consistent with Scheme 1B. From analyses of the MFEs and several theoretical expressions, the rate constants of the decay processes have been estimated.

2. Results and Discussion

2.1. Quenching of ^{3}(2-X)MPTZ* by Electron Acceptors. Figure 1 shows transient absorption spectra on excitation of 2-MeOMPTZ in the presence of TCNB (5×10^{-4} M) in 2-PrOH with a 355 nm laser pulse. Immediately after excitation, a broad absorption band was observed at 485 nm. This band was assigned to the T−T absorption of 2-MeOMPTZ, because its shape was quite similar to that of the T−T absorption band (λ_{max} = 465 nm)[18] of MPTZ, although the λ_{max} value of the former was shifted to the red by 20 nm compared with that of the latter. The T−T absorption decayed within 1 μs with

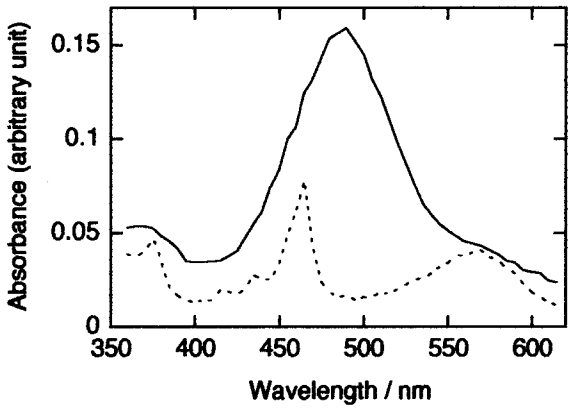

Figure 1. Transient absorption spectra of the 2-PrOH solution of 2-MeOMPTZ (7×10^{-4} M) and TCNB (5×10^{-4} M) at 35 ns (solid line) and 1 μs (dotted line) after excitation at 355 nm.

TABLE 1: Quenching Rate Constants (k_q), Free Energy Changes (ΔG_{ET}, ΔG_{BET}), Free Ion Yields at 0 T (Φ_{FI}), and MFEs for the Reactions of ^{3}(2-X)MPTZ* (^{3}D*) with the Acceptors (A) in 2-PrOH at 293 K

run	D	A	k_q[a]	ΔG_{ET}[b]	ΔG_{BET}[b]	Φ_{FI}[c]	$R(B)_{max}$	$am/(1-\beta)$[d]
1	2-MeOMPTZ	TCNB	6.2	−1.42	−1.22	0.52	1.04	0.95
2	MPTZ	TCNB	6.3	−1.35	−1.29	0.55 (0.93)	1.06	1.04
3	MPTZ	F_4DCNB	5.9	−1.00	−1.64	0.66 (0.96)	1.07[e]	0.99
4	MPTZ	F_4DMTP	4.3	−0.64	−2.00	NA[g]	1.09	NA[h]
5	MPTZ	*p*-DCNB	4.6	−0.39	−2.25	0.71 (0.93)	1.07[e]	1.20
6	MPTZ	MeCNBz	3.9	−0.36	−2.28	0.65[i]	1.09	1.23
7	MPTZ	*o*-DCNB	4.3	−0.33	−2.31	0.63 (0.90)	1.09	1.10
8	MPTZ	DMTP	3.4	−0.32	−2.32	NA[g]	1.13	1.53
8′	MPTZ-d_3	DMTP-d_{10}	*f*	−0.32	−2.32	NA[g]	1.05	*f*
9	2-ClMPTZ	*p*-DCNB	*f*	−0.31	−2.33	0.75 (0.97)	1.08	1.00
10	2-MeOMPTZ	*m*-DCNB	3.5	−0.22	−2.42	0.77	1.10	1.30

[a] Unit = 10^9 M^{-1} s^{-1}. [b] Unit = eV. [c] The estimated error is ±0.05. The values in parentheses are obtained in MeCN. [d] Unit = 10^{-5} $s^{1/2}$. [e] Reference 18. [f] Not determined. [g] Not available due to the overlap of the absorption spectra of $D^{\bullet+}$ and $A^{\bullet-}$. [h] Not available due to lack of the *g*-factor of $A^{\bullet-}$. [i] Reference 44b.

concomitant growth of new bands at 575 and 465 nm. The spectrum recorded at 1 μs after excitation (Figure 1, dotted line) was ascribed to a superposition of the absorption spectra due to 2-MeOMPTZ$^{\bullet+}$ (λ_{max} = 576 and 425 (shoulder) nm in CH_2Cl_2) and TCNB$^{\bullet-}$ (λ_{max} = 462, 436, 414, 375, and 353 nm in MeCN). This spectral change indicates that an electron was transferred from ^{3}(2-MeO)MPTZ* to TCNB. Occurrence of ET from ^{3}D* to A was also observed by the transient spectra for other combinations of D and A listed in Table 1.

To clarify the relationship between the quenching rate constant (k_q) and the free energy change (ΔG_{ET}) accompanying the forward ET, we determined the k_q values from the Stern−Volmer plots. The observed k_q values are listed in Table 1. The ΔG_{ET} value is given by[20]

$$\Delta G_{ET} = -E_{red}(A) + E_{ox}(D) - e^2/(4\pi\epsilon_0\epsilon_r R_{AD}) - E_T \quad (1)$$

where E_{red}(A) and E_{ox}(D) are the half-wave potentials of reduction of A and of oxidation of D in the ground state,[21] respectively, and E_T is the triplet excitation energy of D. The E_T value reported for MPTZ (2.64 eV[22]) was used for all the donors, because the phosphorescence spectra of 2-MeOMPTZ and 2-ClMPTZ recorded at 77 K in a 1:1 mixture of 2-PrOH and EtOH were quite similar to that of MPTZ. The separation distance between $D^{\bullet+}$ and $A^{\bullet-}$ in SSRIP (R_{AD}) was assumed to be 8 Å.[23] The forward ET was exergonic for any reactions investigated with the ΔG_{ET} value ranging from −1.42 to −0.22 eV, as shown in Table 1. The k_q value tended to increase with decreasing ΔG_{ET}, approaching the diffusion-limited value (k_d). Such ΔG_{ET} dependence of k_q has often been observed in bimolecular ET and interpreted by the Rehm−Weller relationship.[20] When the concentration of A was 1×10^{-3} M (the standard condition of our experiments), the lifetime of ^{3}D* was shorter than ca. 280 ns, and more than 95% of ^{3}D* was quenched by A.

Figure 2 shows the time profiles of the transient absorbance, which we refer to as $A(t)$ curves herein, for the reaction of ^{3}MPTZ* with *o*-DCNB monitored at 520 nm. At this wavelength both ^{3}MPTZ* ($\epsilon_{520} = 5.3 \times 10^3$ M^{-1} cm^{-1}) and MPTZ$^{\bullet+}$ ($\epsilon_{520} = 9.2 \times 10^3$ M^{-1} cm^{-1}) absorb light, while *o*-DCNB$^{\bullet-}$ shows no significant absorption. The $A_{520}(t)$ curve was composed of an initial rise ($0 < t <$ ca. 200 ns) and a decay afterward. At a microsecond time region (1 μs $< t <$ 8 μs), the decay of $A_{520}(t)$ obeyed a second-order kinetics, corresponding to bimolecular backward ET between free MPTZ$^{\bullet+}$ and *o*-DCNB$^{\bullet-}$. Similar $A(t)$ curves were observed for other reactions between ^{3}D* and A. These features of the $A(t)$ curves indicate that

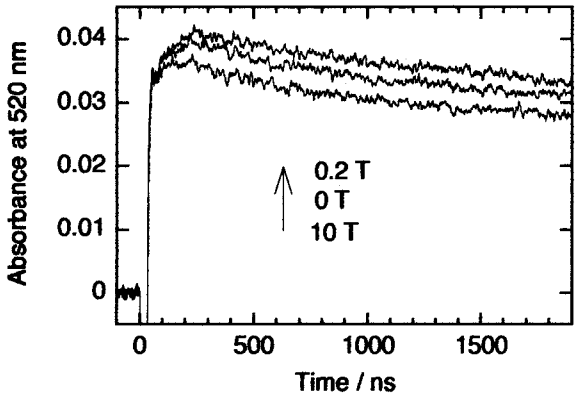

Figure 2. Time profiles of the transient absorbance at 520 nm for the reaction of MPTZ with *o*-DCNB in 2-PrOH under various magnetic fields.

lifetimes of any postulated intermediates (^{3}Ex*, ^{3}CRIP, and SSRIP) are much shorter than the decay time of ^{3}D* (170−280 ns) under the experimental conditions employed and that formation of free ions has been completed within 1 μs. Although the absolute values of the rate constants for the decay processes of these intermediates cannot be determined, the free ion yield (Φ_{FI}) defined by eq 2 is likely to reflect the relative magnitudes of these rates.

$$\Phi_{FI} \equiv [\text{no. of free } D^{\bullet+} \text{ formed}]/[\text{total no. of } ^3D^* \text{ quenched by A}] \quad (2)$$

The denominator of eq 2 was obtained as [no. of ^{3}D* generated by excitation] × k_q[A]/($\tau_T^{-1} + k_q$[A]), where τ_T is the decay rate of ^{3}D* in the absence of A (see Experimental Section).

The Φ_{FI} values obtained for the reactions between ^{3}D* and A in 2-PrOH and MeCN are listed in Table 1. In 2-PrOH, the Φ_{FI} values were greater than 0.5 and tended to increase with increase in ΔG_{ET}, but this correlation was not so clear. In MeCN, which has a higher dielectric constant and a lower viscosity than 2-PrOH, the Φ_{FI} values were higher than the corresponding values observed in 2-PrOH and close to unity. It is noteworthy that the Φ_{FI} values for these reactions in 2-PrOH and MeCN were much higher than those reported for similar charge-separation type ET reactions with singlet precursors in MeCN.[2−6] In most cases with singlet precursors, the Φ_{FI} values were reported to be less than 0.2. Only for the reactions where the backward ET was extremely exergonic ($\Delta G_{BET} \leq$ ca. −2.7 eV) were relatively high values of Φ_{FI} (0.6−0.8) attained.[4a] On the other hand, for ET to the T_1 state of benzophenone from 1,2-

diazabicyclo[2.2.2]octane, the Φ_{FI} value was reported to be unity.[24] For ET to the T_1 states of C_{60} derivatives from *N*,*N*-dimethylaniline in benzonitrile, the Φ_{FI} values were also unity.[17a] Φ_{FI} values for reactions with triplet precursors higher than those with singlet ones are ascribed to the fact that both the deactivation of ^{3}CRIP or ^{3}Ex* to the ground states and the geminate backward ET within ^{3}SSRIP are spin-forbidden, as was mentioned in Introduction. Thus, the spin multiplicity of the precursor can affect the Φ_{FI} value through the decay dynamics of CRIP (or Ex*) and of SSRIP. Assuming that formation of SSRIP from CRIP (or Ex*) is practically irreversible (process b in Scheme 1B),[25] we can present Φ_{FI} by

$$\Phi_{FI} = \phi_{SSRIP}\phi_{sep} \tag{3a}$$

$\phi_{SSRIP} \equiv$ [no. of geminate ^{3}SSRIP formed]/

[total no. of ^{3}D* quenched by A] (3b)

$\phi_{sep} \equiv$ [no. of free $D^{\bullet+}$ formed]/

[no. of geminate ^{3}SSRIP formed] (3c)

The efficiency of SSRIP formation (ϕ_{SSRIP}) is determined by the competition between the processes b and c and the contribution from the long-distance ET (process d). The efficiency of separation to free ions from SSRIP (ϕ_{sep}) is determined by the interplay of the spin conversion (process e), separation to free ions (processes g and G), and backward ET from ^{1}SSRIP (process F). The following sections describe the magnetic field effects, ΔG_{BET} dependence, solvent effects, and heavy atom effects of ϕ_{SSRIP} and ϕ_{sep}.

2.2. MFEs on Free Ion Yields. According to the theory on the radical pair mechanisms of MFEs, magnetic fields can alter the efficiency of spin conversion for remote radical pairs (RPs) but not for contact RPs.[26,27] In remote RPs, the nearly degenerate singlet (S) and triplet (T) states can be interconverted due to the isotropic hyperfine coupling (HFC) and Zeeman interactions, while the S−T conversion for contact RPs is prohibited by large magnitude of exchange interaction ($|J|$). Because the R_{AD} value is considered to be 7−8 Å in SSRIP, this intermediate corresponds to a remote RP. On the other hand, CRIP, where $D^{\bullet+}$ and $A^{\bullet-}$ are located with van der Waals contact ($R_{AD} \sim 4$ Å), corresponds to a contact RP. Thus, only the S−T conversion of SSRIP (process e in Scheme 1B) can be affected by magnetic fields. In other words, ϕ_{sep} is dependent on the magnetic field strength (B), while ϕ_{SSRIP} is independent of B.

To clarify the B dependence of ϕ_{sep}, we examined MFEs on Φ_{FI} for the reactions listed in Table 1 in 2-PrOH in a field range of 0−10 T. Figure 2 shows the $A(t)$ curves for run 7 at different B's. The Φ_{FI} values at $B = 0.2$ and 10 T were higher and lower, respectively, than Φ_{FI} (0 T). To represent the magnitude of MFEs on Φ_{FI}, we use the ratio of transient absorbance in the presence and absence of the magnetic field, $R(B) = A$ (1 μs, B)/A (1 μs, 0 T), which can be regarded as the ratio of $\phi_{sep}(B)/\phi_{sep}$(0 T). Typical plots of $R(B)$ vs $B^{1/2}$ are shown in Figure 3. The $R(B)$ vs $B^{1/2}$ plots for runs 1−10 exhibited common features. Each $R(B)$ value steeply increased with increasing B from 0 to ca. 0.1 T to reach a maximum, $R(B)_{max}$, and was almost constant at $B = 0.1$−0.5 T. The $R(B)_{max}$ value was ca. 1.1 or less in any cases as shown in Table 1. The $R(B)$ value decreased with increase in B from 0.5 to 10 T showing linear relationship with $B^{1/2}$. The observed R(10 T) values were 0.86−0.94.

The observed increase in $R(B)$ with increasing B from 0 to 0.2 T can be explained by the hyperfine coupling mechanism (HFCM).[26] The HFC-induced T−S conversion rate of RP, k_{HFC}, is estimated from the effective HFC of the component radicals, $|A_{HFC}|$ ($=[\Sigma_i a_i^2 I_i(I_i + 1)]^{1/2}$).[28,29]

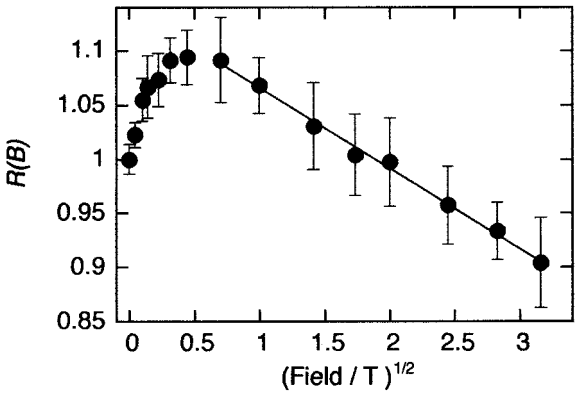

Figure 3. $R(B)$ vs $B^{1/2}$ plots for the reaction of MPTZ with *o*-DCNB in 2-PrOH at 293 K.

$$k_{HFC} = \pi g \mu_B B_{1/2}/h \tag{4a}$$

$$B_{1/2} = 2[|A_{HFC}(1)|^2 + |A_{HFC}(2)|^2]/[|A_{HFC}(1)| + |A_{HFC}(2)|] \tag{4b}$$

The $|A_{HFC}(MPTZ^{\bullet+})|$ value of 1.58 mT[18] is much larger than the $|A_{HFC}|$ value (0.28−0.62 mT) of $A^{\bullet-}$ whose HFC values are available. It is likely that the $|A_{HFC}|$ values of 2-MeOMPTZ$^{\bullet+}$ and 2-ClMPTZ$^{\bullet+}$ are almost the same as or slightly smaller than that of MPTZ$^{\bullet+}$. For the reactions listed in Table 1, the k_{HFC} values estimated by eq 4 fall within a range of $(1.16-1.21) \times 10^8$ s^{-1} except for run 8′. Thus, the similarity in the B dependence of $R(B)$ at $B = 0$−0.1 T among these reactions is consistent with the similarity in k_{HFC} for these SSRIPs.

For runs 8 and 8′, the $A_{520}(t)$ curves were measured for the sample solutions having identical absorbance at 355 nm on excitation with an identical laser intensity. The ratios of A_{520}(run 8′; 1 μs)/A_{520}(run 8; 1 μs) were 1.06 and 1.03 at $B = 0$ and 0.1 T, respectively. The larger Φ_{FI} value for run 8′ than that for run 8 is ascribed to a smaller k_{HFC} value (0.96×10^8 s^{-1}) of the former reaction than the value (1.21×10^8 s^{-1}) of the latter one. At fields much higher than the effective HFC values ($B \gg |A_{HFC}|$), only the T_0 state of ^{3}SSRIP can be converted to ^{1}SSRIP, while the $T_{\pm1}$ states exclusively give free ions. As a result, the difference in Φ_{FI} between runs 8 and 8′ decreases. These deuterium effects confirmed that the T−S conversion of SSRIP is induced mainly by the isotropic HFC interactions at low fields ($B \leq 0.1$ T).

The linear relationship between $R(B)$ and $B^{1/2}$ observed at $B = 0.5$−10 T is characteristic of MFEs due to the Δg mechanism (ΔgM). Theoretically, the relative MFE ($Y_{\Delta gM}$) on the escaped radical yield from ^{3}RP due to the ΔgM is expressed as follows.[18]

$$Y_{\Delta gM}(B) - 1 = -1/3[\alpha m/(1-\beta)](\pi \Delta g \mu_B B/2)^{1/2} \tag{5}$$

Here, α, m, and β are parameters of the Noyes' reencounter function,[31] and Δg is the difference in the isotropic g-factors of the component radicals. In the Noyes' function, α ($0 \leq \alpha \leq 1$) is the recombination probability of ^{1}RP, and β ($0.5 \leq \beta < 1$) is the total probability of at least one encounter of two radicals that separated from a nonreactive encounter.[32] As was pointed out by Kaptein,[31b] β becomes larger (closer to unity) when the viscosity increases. m is expressed by the quantities relevant to the relative diffusive motion and inversely proportional to square root of the frequency of the mutual displacement.[33] To eliminate

the contribution of HFCM to $R(B)$ values, we converted $R(B)$ to $Y_{\Delta g\mathrm{M}}(B)$ using the relation, $Y_{\Delta g\mathrm{M}}(B) = R(B)/R_{\mathrm{calcd}}(B\rightarrow 0.1\ \mathrm{T})$. Here $R_{\mathrm{calcd}}(B\rightarrow 0.1\ \mathrm{T})$ is the extrapolated $R(0.1\ \mathrm{T})$ value calculated by the equation representing the least-squares fitted straight line of $R(B)$ vs $B^{1/2}$ plots ($B = 0.5-10$ T). This procedure had also been used in the previous study.[18] The obtained values of $\alpha m/(1-\beta)$ are given in Table 1. Recently, Wakasa et al. reported that the MFEs on the escaped radical yields due to the ΔgM were saturated at $B \geq 20$ T for the reactions involving with a neutral RP in alcoholic solvents.[34] In their case, the $R(B)$ vs $B^{1/2}$ plots started to deviate upward of the straight lines at $B \sim 4$ T ($R(4\mathrm{T}) = 0.79$), approaching the theoretically predicted asymptotic value of $^2/_3$. In the present case, the $R(B)$ vs $B^{1/2}$ plots were still linearly decreasing at $B = 10$ T, and the $Y_{\Delta g\mathrm{M}}(10\ \mathrm{T})$ values (0.78−0.84) were larger than $^2/_3$. Saturation behavior might be observed at much higher fields, since the Δg values of the present SSRIPs (0.0016−0.0027) are smaller than that of the RP in their study (0.0055).

The results of the MFEs give some information on the rate constants, k_{sep} and k_{BET}. The observation of MFEs due to the HFCM suggests that k_{sep} should be comparable with k_{HFC}. The Tachiya's relation[35,36] gives a separation rate (k_{sep}) of $0.9 \times 10^8\ \mathrm{s}^{-1}$ for SSRIP consisting of $\mathrm{D}^{\bullet+}$ of a radius of 3.5 Å and $\mathrm{A}^{\bullet-}$ of a radius of 3.0 Å with an R_{AD} value of 8 Å in 2-PrOH at 293 K (see section 2.5). This k_{sep} value is the same order of magnitude as the estimated k_{HFC} value ($1.2 \times 10^8\ \mathrm{s}^{-1}$). On the other hand, the observation of MFEs due to the ΔgM suggests that k_{BET} should be comparable to or larger than the $\mathrm{S}-\mathrm{T}_0$ conversion rate, $k_{\mathrm{ST0}}(B)$, given by

$$k_{\mathrm{ST0}}(B) = k_{\mathrm{HFC}} + k_{\Delta g}(B) = k_{\mathrm{HFC}} + \pi\Delta g\mu_{\mathrm{B}}B/h \qquad (6)$$

Here, $k_{\Delta g}(B)$ is the rate of $\mathrm{S}-\mathrm{T}_0$ conversion induced by the isotropic Zeeman interaction. For $\mathrm{D}^{\bullet+}-\mathrm{A}^{\bullet-}$ pairs listed in Table 1, the $k_{\mathrm{ST0}}(10\ \mathrm{T})$ values are calculated to be $(0.7-1.3) \times 10^9\ \mathrm{s}^{-1}$. Thus, the k_{BET} ones are estimated to be of the order of $10^9\ \mathrm{s}^{-1}$ or higher.

If k_{sep} or k_{BET} varies for the various SSRIPs, it is expected that the magnitudes of MFEs are different from each other. The $R(B)_{\mathrm{max}}$ and $\alpha m/(1-\beta)$ values can be used as the measures of the magnitudes of MFEs due to the HFCM and ΔgM, respectively. Although $R(B)_{\mathrm{max}}$ depends on k_{HFC}, the k_{HFC} values for the present series of SSRIPs (runs 1−10 except for run 8′) are almost the same. The $\alpha m/(1-\beta)$ value is independent of Δg, as seen in eq 5. Comparison of $R(B)_{\mathrm{max}}$ and $\alpha m/(1-\beta)$ values among runs 1−10 shows the following features: (i) There is a tendency that the larger $R(B)_{\mathrm{max}}$ is, the larger $\alpha m/(1-\beta)$ is. (ii) Among these reactions, the differences in either $R(B)_{\mathrm{max}}$ or $\alpha m/(1-\beta)$ are not so large in comparison with the experimental errors, ±0.01 for the former or ±10% for the latter. (iii) The magnitude of MFEs exhibits no clear correlation with ΔG_{ET} or ΔG_{BET}. (iv) The reactions of the esters such as F_4-DMTP, MeCNBz, and DMTP show somewhat larger MFEs than those of the nitriles. Feature (i) is understood as follows: For large MFEs to be observed, it is the common requirement for both the HFCM and the ΔgM that a significant fraction of the geminate ^{3}SSRIP should not separate to free ions but undergo backward ET through ^{1}SSRIP. Features (ii) and (iii) may be unexpected results. The parameter α, which is determined by the competition between backward ET (process F) and separation (process G) of ^{1}SSRIP, increases with increase in k_{BET} and approaches unity. As will be discussed in section 2.4, k_{BET} is expected to exhibit a characteristic bell-shaped ΔG_{BET} dependence and to vary by about one order among the present series of ^{1}SSRIPs. A plausible explanation for the lack of correlation between $\alpha m/(1-\beta)$ and ΔG_{BET} is as follows. If the backward ET of ^{1}SSRIP is much faster than the separation and the conversion to ^{3}SSRIP ($k_{\mathrm{BET}} \gg k_{\mathrm{ST0}}(B)$, k_{sep}) in any case, α is close to unity, and no significant difference is observed. Alternatively, variation of m and/or β may make the ΔG_{BET} dependence of α obscure. Indeed, feature (iv) may be understood in terms of the difference in m and/or β. In the radical anions of the esters, the oxygen atoms are probably more negatively charged than the cyano groups in the nitrile radical anions. The substituents with high charge densities may cause strong interactions with the polar solvent molecules. The slower diffusion of either of the component radicals corresponds to the smaller m and the larger β in the Noyes' expression, which gives the larger $\alpha m/(1-\beta)$ value.

2.3. MFEs on Decay Rates of Free Ions. As was mentioned in section 2.1, the free ions' decay obeyed second-order kinetics in the microsecond time region. The apparent bimolecular decay rates, k_2, were determined to be $(1.0-1.9) \times 10^{10}\ \mathrm{M}^{-1}\ \mathrm{s}^{-1}$ at 0 T in 2-PrOH at 293 K. However, understanding of the meaning of k_2 is not straightforward. As is shown in Scheme 1B, the association of free $\mathrm{D}^{\bullet+}$ and $\mathrm{A}^{\bullet-}$ (processes h and H) is regarded as the reverse process of the separation of SSRIP to free ions.[16b] The approximate value of k_{assoc} between $\mathrm{D}^{\bullet+}$ and $\mathrm{A}^{\bullet-}$ at zero ionic strength is obtained as[37]

$$k_{\mathrm{assoc}} = k_{\mathrm{d}}r_{\mathrm{C}}/R_{\mathrm{ET}} \qquad (7)$$

Here, r_{C} ($=\mathrm{e}^2/4\pi\epsilon_0\epsilon_{\mathrm{r}}kT$) is the Onsager distance, and R_{ET} is the reaction radius for the ET reaction between the corresponding $^3\mathrm{D}^*$ and A. From the relationship between k_{q} and ΔG_{ET} shown in Table 1, k_{d} is estimated to be $\geq 6.3 \times 10^9\ \mathrm{M}^{-1}\ \mathrm{s}^{-1}$. With R_{ET} values of 4 Å (R_{AD} in CRIP) and 8 Å (R_{AD} in SSRIP), eq 7 gives k_{assoc} values of 4.4×10^{10} and $2.2 \times 10^{10}\ \mathrm{M}^{-1}\ \mathrm{s}^{-1}$, respectively. The observed k_2 values are lower than the estimated k_{assoc} value, which is at least partially ascribed to the spin selectivity of backward ET.

At random encounter of free radical ions, both ^{3}SSRIP and ^{1}SSRIP are formed in a statistical ratio of 3:1. The behavior of ^{3}SSRIP formed by process h should be the same as that of geminate ^{3}SSRIP, which is formed through the process b and/or process d. Namely, ϕ_{sep} fraction of ^{3}SSRIP separates to give free ions, while the remaining part ($1-\phi_{\mathrm{sep}}$) disappears through the T−S conversion followed by backward ET. On the other hand, most of the ^{1}SSRIP formed through process H decays through backward ET because $k_{\mathrm{BET}} > k_{\mathrm{ST0}}, k_{\mathrm{sep}}$. The observed k_2 value contains a contribution from both ^{1}SSRIP formed through process H and ^{3}SSRIP formed through process h. However, the observed MFEs on k_2 predominantly result from B-dependent behavior of ^{3}SSRIP, because ^{3}SSRIP has a larger initial population and a longer lifetime than ^{1}SSRIP. Accordingly, it is predicted that the k_2 value will exhibit MFE reflecting the B dependence of the separation efficiency of ^{3}SSRIP (ϕ_{sep}). A theoretical study by Werner et al. dealt with MFEs on bimolecular reactions between free radicals more quantitatively.[38] So far, only a few experimental works have been reported for MFEs on such reactions.[18,39] We examined B dependence of k_2 for the same reactions as the investigation of MFEs on Φ_{FI}. Figure 4 shows the $k_2(B)$ vs $B^{1/2}$ plots for the reaction of $\mathrm{MPTZ}^{\bullet+}$ with $\mathrm{TCNB}^{\bullet-}$ (run 2) in 2-PrOH. The k_2 value decreased with increasing B from 0 to 0.5 T, while it increased with B from 1 to 10 T up to ca. 1.2-fold of $k_2(0\ \mathrm{T})$. This B dependence of k_2 is quite similar to that of $R(B)$ (Figure 3), which agrees with the above prediction.

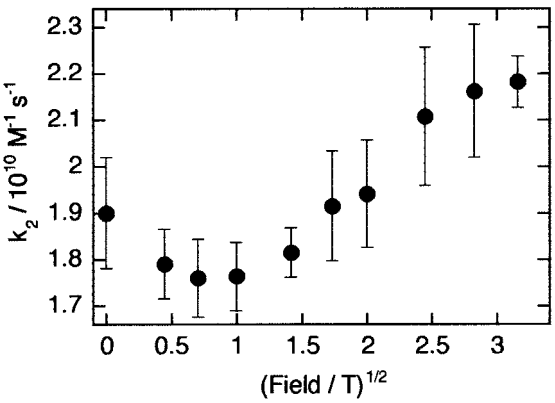

Figure 4. k_2 vs $B^{1/2}$ plots for the reaction of $MPTZ^{\bullet+}$ with $TCNB^{\bullet-}$ in 2-PrOH at 293 K.

TABLE 2: Free Energy Changes of Backward ET (ΔG_{BET}), Phases of CIDEP, and Signs of *J* for SSRIPs Composed of $MPTZ^{\bullet+}$ and $A^{\bullet-}$ in 2-PrOH at 293 K

A	ΔG_{BET} /eV	CIDEP phase	sign of *J*
TCNB	−1.29	E/A[a]	negative
PI	−1.49	E*/A[b]	negative
F_4DCNB	−1.64	A/E[c]	positive
F_4DMTP	−2.00	A/E	positive
p-DCNB	−2.25	A/E	positive
MeCNBz	−2.28	A/E	positive
DMTP	−2.32	A/E	positive

[a] Emission in the low field and absorption in the high field. [b] The emissive signal was stronger than the absorptive one. [c] Absorption in the low field and emission in the high field.

2.4. Energy Gap Dependence of Backward ET Rates. According to the Marcus theory,[40] a nonadiabatic ET rate is expressed by

$$k^M = (4\pi^2/h)V^2(4\pi\lambda kT)^{-1/2}\exp[-(\Delta G + \lambda)^2/4\lambda kT] \quad (8)$$

Here, λ is the total reorganization energy, which consists of the outer-sphere contribution (λ_{out}) and the energy associated with the intramolecular reorganization (λ_{in}). *V* denotes the electronic coupling matrix element. Equation 8 means that k^M is maximized at $-\Delta G = \lambda$ and decreases as ΔG goes farther from this point in both the normal ($-\Delta G < \lambda$) and inverted ($-\Delta G > \lambda$) regions. Although the evaluation of the absolute k^M values requires the knowledge of *V*, the relative magnitudes of k^M within a series of donor−acceptor pairs can be estimated if λ is known. Recently, Kobori et al. proposed a new method to estimate λ for backward ET of SSRIP.[41] According to the perturbation theory, the exchange integral (*J*) of RIP is related to ΔG_{BET} by[42]

$$J \approx -V^2/(\lambda + \Delta G_{BET}) \quad (9)$$

The signs of *J* for SSRIPs can be determined from the phases of multiplet effect of chemically induced dynamic electron polarization (CIDEP) due to the radical pair mechanism, if the spin multiplicities of the reaction precursors are known.[43] They estimated λ accompanying the backward ET to be ca. 1.8 eV for SSRIPs consisting of $MPTZ^{\bullet+}$ and $A^{\bullet-}$ in dimethyl sulfoxide (DMSO), where $A^{\bullet-}$ was the radical anion of the aromatic electron acceptor such as TCNB and *p*-DCNB. We measured CIDEP spectra for the reactions listed in Table 2[44] and estimated the λ value to be 1.5−1.6 eV in 2-PrOH. With a dielectric continuum model, λ_{out} is obtained by[40]

TABLE 3: Viscosity (η), Dielectric Constants (ϵ_r) of Various Solvents, Free Ion Yields (Φ_{FI}), Calculated Separation Rates (k_{Sep}), MFEs for the Reaction of ^{3}MPTZ* with *p*-DCNB at 293 K

solvent	η/cP[a]	ϵ_r[a]	k_{sep}/ 10^8 s^{-1}	Φ_{FI}(0 T)	$R(B)_{max}$	$\alpha m/(1-\beta)$[b]
MeCN	0.37	36.64	18	0.93	1.03	0.49
MeOH	0.61	33.0	9.5	0.93	1.05	*c*
EtOH	1.19	25.3	3.1	0.85	1.06	0.78
2-PrOH	2.20	20.18	1.0	0.71	1.07	1.20
1-BuOH	2.95	17.84	0.53	0.56	1.14	1.24
C_6H_6−DMSO[d]	NA[e]	NA[e]	NA[e]	*c*	1.15	1.51

[a] Reference 63. [b] Unit 10^{-5} $s^{1/2}$. [c] Not measured. [d] Reference 18. [e] Not available.

$$\lambda_{out} = e^2/(8\pi\epsilon_0)(1/r_A + 1/r_D - 2/R_{AD})(1/n^2 - 1/\epsilon_r) \quad (10)$$

where *n* is the refractive index of the solvent. For SSRIP with an R_{AD} value of 8 Å, λ_{out} was calculated to be 1.27 eV in 2-PrOH at 293 K. The λ_{in} values were estimated to be 0.2 and 0.1 eV for $MPTZ^{0/\bullet+}$ and *p*-$DCNB^{0/\bullet-}$ (as a representative of $A^{0/\bullet-}$), respectively, by the method of Nelsen[45] based on AM1[46] calculations. The λ ($=\lambda_{out} + \lambda_{in}$) value was calculated to be 1.57 eV, which agreed with the above value obtained from the CIDEP experiments.

Thus, the backward ET for runs 1−10 in Table 1 covered from the normal to inverted regions. The magnitude of *V* has been reported to be $(1.2-5) \times 10^{-3}$ eV (10−40 cm^{-1}) for typical backward ET within SSRIPs consisting of aromatic radical ions.[3-5] Equation 8 with this range of *V* and the estimated value of λ (1.6 eV) gives a maximum rate (k^M_{max}) of 2×10^{10} - 3×10^{11} s^{-1}. This classical formula, however, predicts that k_{BET} for run 10 will be reduced to about 1/50 of k^M_{max}, which may be smaller than the value estimated in section 2.2. Alternatively, in the semiclassical expression by Bixon and Jortner,[47] the *k* value in the inverted region decreases less steeply than predicted by eq 8. By this semiclassical expression with $\lambda_{out} = 1.27$ eV, $\lambda_{in} = 0.3$ eV, and a typical value of 1500 cm^{-1} for the average energy of the high-frequency intramolecular vibrational modes, the maximum value (k^{BJ}_{max}) is predicted to be by ca. 20% larger than k^M_{max} and the k_{BET} value for run 10 to be about one-tenth of k^{BJ}_{max}. Experimentally obtained k_{BET} values of 10^9 −10^{10} s^{-1} were reported for backward ET reactions in the deeply inverted region ($\Delta G_{BET} = -(2.0-2.3)$ eV).[3b,d,4a,6b] From these facts, the k_{BET} values for the reactions in Table 1 are estimated to be of the order of 10^9 to 10^{11} s^{-1}, which are larger than k_{sep} (9×10^7 s^{-1}) and $k_{ST0}(B)$ (1.1×10^9 s^{-1} at 10 T). This result is consistent with the qualitative consideration described in section 2.2.

2.5. Solvent Effects on MFEs. As was demonstrated in the previous sections, ΔG_{BET} hardly affected on the magnitude of MFEs in the present reactions. Next, we examined the effects of solvent on the MFEs for the reaction with ^{3}MPTZ* with *p*-DCNB. Table 3 shows that both $R(B)_{max}$ and $\alpha m/(1-\beta)$ increased with increase in viscosity (η) and decrease in dielectric constant (ϵ_r) from MeCN to 1-BuOH. With the change of solvent, $R(B)_{max}$ and $\alpha m/(1-\beta)$ varied more largely than with the different reactions in 2-PrOH (Table 1). To elucidate the origin of the solvent effects on MFEs, we must consider how the solvent properties affect the rate constants k_{HFC}, $k_{\Delta g}$, k_{BET}, and k_{sep}. First, the S−T conversion rates, k_{HFC} and $k_{\Delta g}$, are independent of the solvent properties, because the $|A_{HFC}|$ and *g*-factors of $MPTZ^{\bullet+}$ and *p*-$DCNB^{\bullet-}$ are likely almost the same in all the solvents in Table 3. Second, the change in ϵ_r alters k_{BET} through ΔG_{BET} and λ_{out} (see eqs 1, 8, and 10). With an increase in ϵ_r from 1-BuOH to MeCN, ΔG_{BET} slightly (by less

than 0.08 eV) increases, λ_{out} increases by 0.19 eV, and as a result k_{BET} increases. As was described in section 2.2, the increase in k_{BET} could enhance the MFEs. However, the observed solvent effect is opposite, indicating that the variation in k_{BET} among these solvents has no substantial effect on the magnitude of MFEs. This is similar situation to the lack of ΔG_{BET} dependence for the reactions in 2-PrOH.

Thus, k_{HFC}, $k_{\Delta g}$, and k_{BET} are not important factors of the observed solvent effects. On the other hand, k_{sep} significantly depends on η and ϵ_r of the solvent. Several experimental studies have reported that k_{sep} values are $(0.5-2) \times 10^9$ s^{-1} for SSRIPs composed of univalent aromatic radical ions in MeCN.[48] For the other solvents, experimental data are not available. According to the theory of Sano and Tachiya, k_{sep} of an ion pair $[D^+-A^-]$ is expressed by[35]

$$k_{sep} = Dr_C/[R_{AD}{}^3\{\exp(r_C/R_{AD}) - 1\}] \qquad (11)$$

Here, D is the mutual diffusion coefficient, which is expressed as $kT\,(1/r_A + 1/r_D)/6\pi\eta$ by the Stokes−Einstein relationship. The k_{sep} value of 1.8×10^9 s^{-1} calculated for MeCN by eq 11 falls within the range of above-mentioned experimental values. As is seen in Table 3, $\Phi_{FI}(0\ T)$ increases with an increase in k_{sep}. This is mainly attributed to an increase in $\phi_{sep}(0\ T)$, although ϕ_{SSRIP} may also increase with increasing ϵ_r.[49] Both $R(B)_{max}$ and $\alpha m/(1-\beta)$ values showed clear correlation with k_{sep}. The $R(B)_{max}$ value increased with a decrease in k_{sep}, indicating that the magnitude of MFEs due to the HFCM is mainly determined by the relative magnitudes of k_{sep} and k_{HFC}. The $\alpha m/(1-\beta)$ value increases with a decrease in k_{sep}, which can be explained by the Noyes' reencounter model; that is, the smaller k_{sep} corresponds to the larger β.[31] More quantitative consideration may be possible. In MeCN, where k_{sep} is much larger than k_{HFC} (1×10^8 s^{-1}), MFE due to the HFCM was hardly observed, but a small magnitude of MFE due to the ΔgM was observed. This seems reasonable because $k_{ST0}(B)$ increases with an increase in B, reaching 1.1×10^9 s^{-1} at $B = 10$ T, which is comparable to k_{sep}. In 2-PrOH, the k_{sep} value is smaller than that in MeCN and comparable to or somewhat larger than k_{HFC}.[50] At $B = 10$ T, where k_{sep} is much smaller than $k_{ST0}(B)$, a large fraction of ^{3}SSRIP born in the T_0 sublevel is converted to ^{1}SSRIP, which immediately decays through backward ET. Thus, MFEs due to both the HFCM and ΔgM are expected to be observable, which is consistent with the experimental results. Table 3 shows that the magnitudes of MFEs in a mixed solvent of benzene and DMSO (3:1 v/v) were larger than those observed in any single solvent. It is likely that the preferential solvation[51] of SSRIP inhibits the separation to free ions in this binary solution, because DMSO has a much stronger ability to stabilize ions than benzene. Thus, the observed solvent effects on MFEs are mainly attributed to the variation in k_{sep} with η and ϵ_r of the solvents.

2.6. Heavy Atom Effects on the Quenching Pathways. Heavy atom effects on ET reactions involving triplet excited molecules have been reported.[15,16] In these reactions, introduction of a heavy atom into the donor or acceptor reduced free radical yields because the intermediate with the triplet spin multiplicity was partially deactivated to the singlet ground states. In quenching of singlet excited states through the charge-transfer process, heavy atom effects were also observed as an enhancement of the intersystem crossing of ^{1}CRIP or ^{1}Ex* to give the locally excited triplet state.[3b,52] The acceleration of these spin-forbidden processes has been explained by the spin−orbit coupling (SOC).[53] Since SOC is a short-range interaction, the presence of a heavy atom affects the decay processes of CRIP or Ex* more markedly than those of SSRIP. Kikuchi et al. utilized the heavy atom effects as diagnostic for the intermediacy of ^{1}Ex* in the ET reactions involving the singlet excited states.[3b]

TABLE 4: Reduction Potentials (E_{Red}) of the Acceptors (A) in MeCN and ΔG_{ET}, k_q, and Φ_{FI} for the Reactions of ^{3}MPTZ* with A in 2-PrOH at 293 K

run	A	E_{red}/V[a]	ΔG_{ET}/eV	$k_q/10^9$ M^{-1} s^{-1}	Φ_{FI}[b]
11	F_5BN	−2.02 [c]	−0.395	3.3	0.26 (0.97)
11B	BrF_4BN	−1.60 [c]	−0.815	4.3	∼0 (0.26)
5	*p*-DCNB	−2.02[d]	−0.395	4.6	0.71 (0.93)
5B	BrDCNB	−1.73[c]	−0.685	5.0	0.34 (NA[e])
8	DMTP	−2.095[d]	−0.32	3.4	NA[f]
8B	BrDMTP	−1.89[c]	−0.525	4.2	NA[f]

[a] Versus ferrocene. [b] The estimated error is ±0.05. The values in parentheses are obtained in MeCN. [c] Determined by normal pulse voltammetry. The estimated error is ±10 mV. [d] Determined by cyclic voltammetry. The estimated error is ±5 mV. [e] Not available because of the instability of $A^{\bullet-}$. See ref 59. [f] Not available due to the overlap of the absorption spectra of $D^{\bullet+}$ and $A^{\bullet-}$. Relatively, Φ_{FI} (run 8) > Φ_{FI} (run 8B).

To clarify whether ^{3}CRIP or ^{3}Ex*[54] is formed as an intermediate in the reactions of ^{3}(2-X)MPTZ* with A in 2-PrOH, we examined the quenching of ^{3}MPTZ* with acceptors containing a Br atom. As is shown in Table 4, the Φ_{FI} values for the Br-substituted acceptors (runs 11B and 5B) were lower than those for the corresponding F-substituted or unsubstituted acceptors (runs 11 and 5, respectively). Although the absolute values of Φ_{FI} for runs 8 and 8B were not obtained due to the overlap of the absorption bands of $MPTZ^{\bullet+}$ and $(Br)DMTP^{\bullet-}$, comparison of the transient absorbance assigned to the free ions indicated that the Φ_{FI} value for run 8B was smaller than that for run 8. The decrease in Φ_{FI} by introduction of a Br atom can be attributed to decrease in ϕ_{SSRIP} due to the SOC-induced deactivation of ^{3}CRIP to the singlet ground states (process c). It is likely that the ϕ_{sep} values for the SSRIPs containing Br atoms (runs 5B, 8B, and 11B) are almost the same as those for the corresponding SSRIPs with no Br atom (runs 5, 8, and 11), because the effect of the SOC interaction in SSRIPs are small, as mentioned before. Thus, the observation of heavy atom effects revealed that the geminate ^{3}SSRIP is formed at least partially through the solvation of ^{3}CRIP (process b).

It has been reported for ET quenching of a molecule in a singlet excited state that large heavy atom effects have been observed only at low exergonicity ($\Delta G_{ET} > -0.4$ eV) where the primary product is not a ^{1}SSRIP but a ^{1}CRIP.[3] In the present case, however, runs 11B, 5B, and 8B whose exergonicities were higher than the above criterion (see Table 4) showed significant heavy atom effects, in contrast to the singlet quenching. At the present state, we cannot discuss ΔG_{ET} dependence of heavy atom effects, because we examined only three reactions whose ΔG_{ET} values change only by 0.3 eV. Although the origin of the difference between the quenching of ^{3}MPTZ* and the ET quenching in the singlet manifold is unclear, solvation of ^{3}CRIP by 2-PrOH might be much slower than the SOC-induced back charge-transfer, or the primary quenching product might be ^{3}Ex* with large resonance stabilization. In MeCN, the Φ_{FI} values for the Br-substituted acceptors were higher than those observed in 2-PrOH. Because k_{solv} in MeCN is probably larger than that in 2-PrOH, ^{3}CRIP gives ^{3}SSRIP more efficiently than in 2-PrOH. Furthermore, the contribution of direct formation of ^{3}SSRIP through long-distance ET (process d) in MeCN may be larger than in 2-PrOH.

Comparison of runs 11B and 5B suggests that the SOC-induced deactivation with BrF_4BN is more effective than that

with BrDCNB, although either of the acceptor molecules contains one Br atom. According to Steiner et al.,[12,52] the probability of SOC-induced spin-forbidden backward ET is proportional to the spin density at the heavy atom. UB3LYP/6-31+G(d)//UHF/3-21G calculations showed that the absolute value of spin density at the Br atom in $BrF_4BN^{\bullet-}$ (0.013) is higher than that in $BrDCNB^{\bullet-}$ (0.001), which can explain the larger heavy atom effect for run 11B than that for run 5B.

2.7. Kinetic Behaviors of ^{3}CRIP and Evaluation of ϕ_{SSRIP}. As was discussed in the previous sections, both ^{3}CRIP and ^{3}SSRIP were involved in ET from ^{3}(2-X)MPTZ* to A in 2-PrOH. In ET reactions with singlet precursors (Scheme 1A), it has been discussed which (or both) of processes C and F contributes the geminate deactivation to the ground states, and experimental determination of k_g and k_{BET} has been attempted.[4d,g,5,6a,25b]

In the present ET reactions, the kinetic behaviors of ^{3}CRIP and ^{3}SSRIP cannot be observed directly, but they are considered to be reflected in ϕ_{SSRIP} and ϕ_{sep}, respectively. The results of the MFEs provide information on a plausible range of the ϕ_{SSRIP} value as follows. On the basis of the theory of the ΔgM (section 2.2), if we assume that the asymptotic value of $Y_{\Delta gM}(B)$ is $^2/_3$ at $B \rightarrow \infty$, we get an inequality, $^2/_3 < \phi_{sep}(B) < 1$ at a range of $0 < B \leq 10$ T. Substitution of eq 3a to this inequality gives a possible range of ϕ_{SSRIP} as $\Phi_{FI}(B)_{max} < \phi_{SSRIP} < \Phi_{FI}(10\ T) \times {}^3/_2$, where $\Phi_{FI}(B)_{max}$ denotes the maximal value of $\Phi_{FI}(B)$ and equals $\Phi_{FI}(0\ T) \times R(B)_{max}$. From this relationship, $0.54 < \phi_{SSRIP} < 0.74$ and $0.84 < \phi_{SSRIP} < 1.0$ were obtained for run 1 and run 10, respectively. As for other reactions, the estimated ranges of ϕ_{SSRIP} fall between the ranges for runs 1 and 10. Although more accurate ϕ_{SSRIP} values cannot be obtained at the present stage, it is likely that ϕ_{SSRIP} values in some reactions, e.g., run 1, are less than unity. This result suggests that a part of ^{3}CRIP should be deactivated to the ground-state instead of being solvated to give ^{3}SSRIP even in the reactions with the acceptors having no Br atom. When the driving force of ET is very large as in run 1, long-distance ET may take place to give ^{3}SSRIP directly to increase ϕ_{SSRIP}.[55] However, the ϕ_{SSRIP} value for run 10 is estimated to be higher than that for run 1, indicating that the contribution of process d is not large. The larger number of cyano groups in TCNB than that in *m*-DCNB may cause a larger magnitude of SOC. Alternatively, even if the effective magnitudes of SOC are the same for runs 1 and 10, the smaller energy gap for run 1 may induce the faster deactivation.[56]

3. Conclusion

The present study has clearly demonstrated that investigation of MFEs on free ion yields (Φ_{FI}) provides unique information on quenching mechanism of excited molecules by various quenchers, especially on dynamic behaviors of intermediates. In the quenching of ^{3}(2-X)MPTZ* by the electron acceptors in 2-PrOH, the reaction pathways are represented by Scheme 1B, which are qualitatively similar to those reported for bimolecular ET reactions with singlet precursors in polar solvents (Scheme 1A). Two kinds of geminate radical ion pairs, ^{3}CRIP and ^{3}SSRIP, are sequentially formed as the intermediates. In the quenching by the Br-substituted acceptors, a significant fraction of ^{3}CRIP was deactivated to the singlet ground states (process c) due to the large magnitude of SOC, decreasing the efficiency of formation of SSRIP (ϕ_{SSRIP}). In the quenching by acceptors having no heavy atom, this process had only minor contribution. SSRIP decayed through the separation to free ions (processes g and G) and the backward ET in the singlet channel (process F). The T−S conversion of SSRIP (process e) was affected by magnetic fields to cause MFEs on Φ_{FI}. The k_{BET} values of ^{1}SSRIP were estimated to be $\geq 1 \times 10^9\ s^{-1}$ even in the highly exergonic cases ($\Delta G_{BET} \sim -2.4$ eV), which is larger than k_{sep} and k_{ST0}. As a result, the relative magnitudes of k_{sep}, k_{HFC}, and $k_{\Delta g}$ mainly determines which mechanism and what magnitude of MFEs are observed. The effects of viscosity and polarity of solvents on k_{sep} is clearly brought out in the MFE experiments.

4. Experimental Section

4.1. Materials. MeOH, EtOH, 2-PrOH (Cica-Merck, HPLC grade), MeCN (Uvasol, spectroscopic grade), and 1-BuOH (Kanto Chemicals, analytical grade) were used as solvents for laser flash photolyses without further purification. MPTZ, 1,2,4,5-tetracyanobenzene (TCNB), and dicyanobenzenes (*o*,*m*,*p*-DCNB, F_4DCNB) were recrystallized from EtOH. Dimethyl terephthalate (DMTP) and methyl 4-cyanobenzoate (MeCNBz) were recrystallized from C_6H_6−hexane. Pentafluorobenzonitrile (F_5BN) (Tokyo Kasei, Co, 99%) and 4-bromo-2,3,5,6-tetrafluorobenzonitrile (BrF_4BN) (Aldrich) were used as received. *N*,*N*′-Dihexylpyromellitdiimide (PI) was obtained in a previous work.[44c] Perchlorate salts of radical cations of MPTZ and 2-ClMPTZ were prepared by the method of Fujita and Yamauchi.[57] 2-MeOMPTZ$^{\bullet+}$ was generated in situ by addition of a known amount of 2-ClMPTZ$^{\bullet+}$(ClO_4^-) to a solution of an excess amount of 2-MeOMPTZ in anhydrous CH_2Cl_2 for the measurements of visible and EPR spectra. The radical anions of the acceptors were prepared in MeCN by the reported procedures.[44c]

4.2. Steady-State Spectroscopy. UV−vis spectra were obtained on a Hitachi U-3210 spectrophotometer. Fluorescence and phosphorescence spectra were recorded on a Shimadzu RF510 spectrofluorometer equipped with a quantum counter. The sample solutions were degassed by bubbling with Ar for 20 min before measurements of the fluorescence spectra. The quantum yields of fluorescence were determined at 293 K with quinine sulfate ($\Phi = 0.546$)[58] as the standard. The phosphorescence spectra were measured at 77 K in a glassy matrix of EtOH−2-PrOH (1:1 v/v). EPR spectra were recorded at room temperature with 100-kHz modulation on an X-band EPR spectrometer (JEOL, JES-RE1X). The magnetic field and the microwave frequency were determined with an NMR field meter (Echo Electronics, EFM-2000AX) and a microwave counter (Echo Electronics, EMC-14), respectively. Perchlorate salts of MPTZ$^{\bullet+}$ and 2-ClMPTZ$^{\bullet+}$ were dissolved to dehydrated CH_2Cl_2 (Organics), and the solutions (3×10^{-4} M) were degassed by five freeze−pump−thaw cycles. The EPR spectra of radical anions were recorded in MeCN immediately after preparation. The microwave power was 0.8 mW.

4.3. Electrochemistry. Cyclic voltammetry was carried out for each sample [$(2-5) \times 10^{-4}$ M] in dehydrated MeCN (Organics) or 2-PrOH containing 0.1 M ^{n}Bu$_4$NBF$_4$ as the supporting electrolyte under an Ar atmosphere with a BAS CV-1B voltammetry controller. Normal pulse voltammetry was performed with a potentiostat (Hokuto Denko, HA-501) controlled by a function generator (Nippon Filcon, JJ-JOKER E-1) with a step height of 10 mV, a pulse width of 40 ms, and a pulse interval of 1 s under an Ar atmosphere. Glassy carbon, Pt wire, and Ag/Ag^+ were used as working, counter, and reference electrodes, respectively. Ferrocene was used as an internal standard.

4.4. Laser Flash Photolyses. All the measurements were carried out at 293 K. Each of the sample solutions was bubbled with nitrogen gas before and during experiments. The solution

flowed through a quartz cell. The magnetic fields of 0−1.7 and 0−10 T were generated by a Tokin SEE-10W electromagnet and an Oxford 37057 superconducting magnet, respectively. The third (355 nm) harmonic of a Quanta-Ray GCR-103 Nd:YAG laser was used as excitation light. The bimolecular quenching rate (k_q) and the lifetime of ^{3}(2-X)MPTZ* in the absence of acceptor (τ_T) were determined by Stern−Volmer plots in a concentration range of 3×10^{-4} to 1.5×10^{-3} M for each acceptor. For measurements of transient absorption spectra and MFEs, the concentrations of MPTZ, 2-ClMPTZ, and 2-MeOMPTZ were 1×10^{-3}, 3×10^{-4}, and 7×10^{-4} M, respectively. The initial concentration of ^{3}(2-X)MPTZ* generated by a laser pulse was about 1×10^{-5} M. A concentration of 1×10^{-3} M was used for each of the acceptors except for TCNB (5×10^{-4} M). Under these conditions, most of ^{3}(2-X)-MPTZ* (≥95%) reacted with the acceptor. On excitation of 2-ClMPTZ, an irreversible reaction was found to occur. In the reactions with the Br-containing acceptors, the radical anions were unstable.[59] For these cases, the sample solution was subjected to only one laser pulse.

4.5. Determination of Φ_{FI}. For each sample solution containing (2-X)MPTZ (D) and an acceptor (A), $A(t)$ curves were recorded every 5 nm in 365−600 nm. The obtained time-resolved transient spectra ($t = 30-1900$ ns) were analyzed with *PCPro-K*[60] based on the following kinetic scheme, where the steady-state condition was assumed for CRIP and SSRIP.

$$^3D^* + A \rightarrow D^{\bullet+} + A^{\bullet-} \quad (12a)$$

$$D^{\bullet+} + A^{\bullet-} \rightarrow D + A \quad (12b)$$

The least-squares fitting afforded the rate constants and the calculated component spectra of ^{3}D* [$A_T(\lambda)$] and radical ions [$A_{RI}(\lambda)$], which is 1:1 superposition of the spectrum of $D^{\bullet+}$ and that of $A^{\bullet-}$. The free ion yield (Φ_{FI}) can be obtained by

$$\Phi_{FI} = [A_{RI}(\lambda_1)/\epsilon_{RI}(\lambda_1)]/[A_T(\lambda_2)/\epsilon_T(\lambda_2)](\tau_T{}^{-1} + k_q[A])/k_q[A] \quad (13)$$

where $\epsilon_{RI}(\lambda_1)$ and $\epsilon_T(\lambda_2)$ are the molar extinction coefficients of the radical ions and ^{3}D*, respectively. The following values were used: for MPTZ, $\epsilon_{RI}(515) = 9.7 \times 10^3$, $\epsilon_T(465)$[22] $= 2.3 \times 10^4$; for 2-ClMPTZ, $\epsilon_{RI}(525) = 1.0 \times 10^4$, $\epsilon_T(475) = 2.1 \times 10^4$; for 2-MeOMPTZ, $\epsilon_{RI}(570) = 1.13 \times 10^4$, $\epsilon_T(485) = 2.3 \times 10^4$ M^{-1} cm^{-1}. The ϵ_T values of 2-XMPTZ were determined by comparison of the T−T absorption intensity at the maximum wavelength with that of the 2-PrOH solution of MPTZ with the identical optical density at 355 nm on excitation with the same laser intensity. The quantum yields for the intersystem crossing were assumed to be the same as that of MPTZ.

4.6. TREPR Spectrometry. TREPR measurements were carried out at room temperature on an X-band pulsed EPR spectrometer (JEOL, RSV2000) in a continuous wave mode without field modulation. The time profiles of transient signal intensities were accumulated for a delay time of 0−3.5 μs after excitation at each magnetic field using a computer-controlled system. The microwave power was 2−5 mW. Each of the sample solutions was deaerated by bubbling with nitrogen gas and flowed through a quartz flat or cylindrical cell with a flow rate of ca. 1.5 cm^3 min^{-1}. The sample was excited with the third harmonic (355 nm) of a Quanta-Ray GCR-3 Nd:YAG laser with a repetition rate of 30 Hz. The concentration of MPTZ and the acceptor were 1×10^{-3} M except for TCNB (5×10^{-4} M) and PI (7×10^{-4} M).

4.7. Quantum Chemical Calculations. The spin densities of the radical anions were calculated by single-point hybrid DFT methods (UB3LYP) with the basis set of 6-31+G(d) for H, C, and N, 6-311+G(d) for Br, and 6-31+G† for F using the geometries optimized at UHF/3-21G level. The spin density of each atom was obtained by the Mulliken's population analysis. For the check of validity of these calculations, the same level of calculations was also carried out for the radical anion of benzonitrile. The calculated isotropic Fermi contact HFC values were $a_{13C}(C{\equiv}N) = -0.541$ (0.612), $a_N = 0.273$ (0.215), $a_H(o) = -0.387$ (0.363), $a_H(m) = 0.025$ (0.030), and $a_H(p) = -0.969$ (0.842) mT, which reproduced the experimental values (shown in parentheses[61]) rather well. These calculations were carried out with Gaussian 98 program[62] on a Fujitsu VPP700E supercomputer at RIKEN. The AM1 calculations were carried out with WinMOPAC ver. 1.

Acknowledgment. E.S. thanks Professor Yasuro Ikuma of Kanagawa Institute of Technology for his continuous interest and encouragement. We thank Dr. Masatoshi Igarashi of RIKEN for his help with the experiments with a superconducting magnet. Thanks are also due to Dr. Kiminori Ushida of RIKEN for invaluable advice on the ab initio calculations. This work was supported by MR Science Project (Chemical Dynamics) of RIKEN.

Supporting Information Available: Synthetic procedures and spectral data for 2-MeOMPTZ and some of the acceptors (PDF). This material is available free of charge via the Internet at http://pubs.acs.org.

References and Notes

(1) *Electron Transfer: from Isolated Molecules to Biomolecules. Part I & II*; Bixon, M., Jortner, J., Eds.; Wiley: New York, 1999.

(2) (a) Mataga, N.; Shioyama, H.; Kanda, Y. *J. Phys. Chem.* **1987**, *91*, 314. (b) Mataga, N.; Asahi, T.; Kanda, Y.; Okada, T. *Chem. Phys.* **1988**, *127*, 249. (c) Ojima, S.; Miyasaka, H.; Mataga, N. *J. Phys. Chem.* **1990**, *94*, 4147, 5834, 7534.

(3) (a) Kikuchi, K.; Takahashi, Y.; Koike, K.; Wakamatsu, K.; Ikeda, H.; Miyashi, T. *Z. Phys. Chem. N. F.* **1990**, *167*, 27. (b) Kikuchi, K.; Hoshi, M.; Niwa, T.; Takahashi, Y.; Miyashi, T. *J. Phys. Chem.* **1991**, *95*, 38. (c) Kikuchi, K.; Takahashi, Y.; Hoshi, M.; Niwa, T.; Katagiri, T.; Miyashi, T. *J. Phys. Chem.* **1991**, *95*, 2378. (d) Kikuchi, K.; Niwa, T.; Takahashi, Y.; Ikeda, H.; Miyashi, T. *J. Phys. Chem.* **1993**, *97*, 5070. (e) Niwa, T.; Kikuchi, K.; Matsusita, N.; Hayashi, M.; Katagiri, T.; Takahashi, Y.; Miyashi, T. *J. Phys. Chem.* **1993**, *97*, 11960. (f) Inada, T. N.; Miyazawa, C. S.; Kikuchi, K.; Yamauchi, M.; Nagata, T.; Takahashi, Y.; Ikeda, H.; Miyashi, T. *J. Am. Chem. Soc.* **1999**, *121*, 7211.

(4) (a) Gould, I. R.; Ege, D.; Moser, J. E.; Farid, S. *J. Am. Chem. Soc.* **1990**, *112*, 4290. (b) Gould, I. R.; Noukakis, D.; Gomez-Jahn, L.; Young, R. H.; Goodman, J. L.; Farid, S. *Chem. Phys.* **1993**, *176*, 439. (c) Gould, I. R.; Young, R. H.; Mueller, L. J.; Farid, S. *J. Am. Chem. Soc.* **1994**, *116*, 8176. (d) Arnold, B. R.; Noukakis, D.; Farid, S.; Goodman, J. L.; Gould, I. R. *J. Am. Chem. Soc.* **1995**, *117*, 4399. (e) Arnold, B. R.; Farid, S.; Goodman, J. L.; Gould, I. R. *J. Am. Chem. Soc.* **1996**, *118*, 5482. (f) Gould, I. R.; Farid, S. *Acc. Chem. Res.* **1996**, *29*, 522. (g) Arnold, B. R.; Atherton, S. J.; Farid, S.; Goodman, J. L.; Gould, I. R. *Photochem. Photobiol.* **1997**, *65*, 15.

(5) (a) Peters, K. S.; Lee, J. *J. Phys. Chem.* **1992**, *96*, 8941. (b) Peters, K. S.; Lee, J. *J. Am. Chem. Soc.* **1993**, *115*, 3643. (c) Li, B.; Peters, K. *J. Phys. Chem.* **1993**, *97*, 13145.

(6) (a) Vauthey, E.; Högemann, C.; Allonas, X. *J. Phys. Chem. A* **1998,** *102*, 7362. (b) Vauthey, E. *J. Phys. Chem. A* **2000**, *104*, 1804.

(7) Yabe, T.; Kochi, K. *J. Am. Chem. Soc.* **1992**, *114*, 4491.

(8) Latterini, L.; Elisei, F.; Aloisi, G. G.; Rodgers, M. A. J. *J. Phys. Chem. A* **1997**, *101*, 9870.

(9) (a) Schael, F.; Löhmannsröben, H.-G. *J. Photochem. Photobiol. A: Chem.* **1997**, *105*, 317. (b) Kircher, T.; Löhmannsröben, H.-G. *Phys. Chem. Chem. Phys.* **1999**, *1*, 3987.

(10) In some cases, Ex* undergoes ET to give CRIP, which is then transformed to SSRIP. Kavarnos, G. J.; Turro, N. J. *Chem. Rev.* **1986**, *86*, 401.

(11) Zhu, Q. Q.; Schnabel, W. *J. Photochem. Photobiol. A: Chem*. **2000**, *130*, 119 and references therein.

(12) (a) Rathore, R.; Hubig, S. M.; Kochi, J. K. *J. Am. Chem. Soc*. **1997**, *119*, 11468. (b) Bockman, T. M.; Hubig, S. M.; Kochi, J. K. *J. Am. Chem. Soc*. **1998**, *120*, 2826.

(13) (a) Hamanoue, K.; Nakayama, T.; Asada, S.; Ibuki, K. *J. Phys. Chem*. **1992**, *96*, 3736. (b) Hamanoue, K.; Nakayama, T.; Sasaki, H.; Ikenaga, K.; Ibuki, K. *Bull. Chem. Soc. Jpn*. **1992**, *65*, 3141.

(14) Jones, G., II.; Mouli, N.; Haney, W. A.; Bergmark, W. R. *J. Am. Chem. Soc*. **1997**, *119*, 8788.

(15) (a) Steiner, U.; Winter, G. *Chem. Phys. Lett*. **1978**, *55*, 364. (b) Ulrich, T.; Steiner, U. E.; Föll, R. E. *J. Phys. Chem*. **1983**, *87*, 1873.

(16) (a) Tamura, S.-I.; Kikuchi, K.; Kokubun, H.; Weller, A. *Z. Phys. Chem. N. F*. **1980**, *121*, 165. (b) Kikuchi, K.; Hoshi, M.; Abe, E.; Kokubun, H. *J. Photochem. Photobiol. A: Chem*. **1988**, *45*, 1.

(17) (a) Luo, C.; Fujitsuka, M.; Huang, C.-H.; Ito, O. *J. Phys. Chem. A* **1998**, *102*, 8716. (b) Komamine, S.; Fujitsuka, M.; Ito, O. *Phys. Chem. Chem. Phys*. **1999**, *1*, 4745. (c) El-Kemary, M.; El-Khouly, M.; Fujitsuka, M.; Ito, O. *J. Phys. Chem. A* **2000**, *104*, 1196.

(18) Sakaguchi, Y.; Hayashi, H. *J. Phys. Chem. A* **1997**, *101*, 549.

(19) (a) Igarashi, M.; Sakaguchi, Y.; Hayashi, H. *Chem. Phys. Lett*. **1995**, *243*, 545. (b) Sakaguchi, Y.; Hayashi, H. *Chem. Phys. Lett*. **1995**, *245*, 591. (c) Wakasa, M.; Hayashi, H. *J. Phys. Chem*. **1996**, *100*, 15640. (d) Kitahama, Y.; Murai, H. *Chem. Phys*. **1998**, *238*, 429.

(20) Rehm, D.; Weller, A. *Isr. J. Chem*. **1970**, *8*, 259.

(21) When the solvent is different from that used in the measurements of redox potentials, the difference in solvation energy is often corrected by adding the term $e^2/(4\pi\epsilon_0)(1/2)(1/r_A + 1/r_D)(1/\epsilon_r - 1/\epsilon_r^s)$, where ϵ_r and ϵ_r^s are the dielectric constants of the solvents used for the ET reaction and the redox potential measurements, respectively. This formula gives a correction term of +90 mV for 2-PrOH vs MeCN. However, the redox potentials measured in 2-PrOH for some of the donors and acceptors agreed with the corresponding values in MeCN within ±10 mV, and the quantity $[E_{red}(A) - E_{ox}(D)]_{2\text{-PrOH}} - [E_{red}(A) - E_{ox}(D)]_{MeCN}$ amounted +(5−15) mV. Accordingly, we used the redox potentials obtained in MeCN without the correction term for calculation of ΔG values of all the reactions in Table 1.

(22) Moroi. Y.; Braun, A. M.; Grätzel, M. *J. Am. Chem. Soc*. **1979**, *101*, 567.

(23) In the present cases, the primary ET intermediate may be CRIP rather than SSRIP. However in 2-PrOH and solvents of higher polarity, the Coulombic interaction is small (∼0.1 eV). Furthermore, evaluation of the free energy change accompanying formation of CRIP is difficult, because the stabilization due to the solvation of each component ion in CRIP is likely less than that in SSRIP. Therefore, we regard the difference in free energy between ^{3}D* plus A and SSRIP as the free energy change accompanying the forward ET (ΔG_{ET}).

(24) Henseler, A.; Vauthey, E. *J. Photochem. Photobiol. A: Chem*. **1995**, *91*, 7.

(25) (a) According to Gould et al., in polar solvents SSRIP is more stable than CRIP and k_{solv} is larger than k_{-solv}.[4d,e,g,25b] For the RIP composed of TCNB$^{\bullet-}$ and the radical cation of *p*-xylene in pentanenitrile, whose dielectric constant (20.2) is similar to that of 2-PrOH (20.18), k_{solv} and k_{-solv} were reported to be 2.6×10^9 and 7×10^8 s^{-1}, respectively. For an ion pair composed of diphenylmethyl cation and Cl$^-$ in MeCN, Peters and Li reported a similar k_{solv} value (2.9×10^9 s^{-1}) and a smaller k_{-solv} value (1.3×10^8 s^{-1}).[25b] For intramolecular RIPs[25c,d] and RIPs in less polar solvents,[25e,f] the reversible transformation between CRIP (or Ex*) and SSRIP plays an important role in their decay processes. (b) Peters, K. S.; Li, B. *J. Phys. Chem*. **1994**, *98*, 401. (c) Bhattacharyya, K.; Chowdhury, M. *Chem. Rev*. **1993**, *93*, 507. (d) De, R.; Fujiwara, Y.; Haino, T.; Tanimoto, Y. *Chem. Phys. Lett*. **1999**, *315*, 383. (e) Aich, S.; Basu, S. *J. Phys. Chem. A* **1998**, *102*, 722. (f) Sengupta, T.; Aich, S.; Basu, S. *J. Phys. Chem. B* **1999**, *103*, 3784.

(26) Hayashi, H. *Dynamic Spin Chemistry*; Nagakura, S., Hayashi, H., Azumi, T., Eds.; Kodansha−Wiley: Tokyo and New York, 1998.

(27) Steiner, U. E.; Ulrich, T. *Chem. Rev*. **1989**, *89*, 51.

(28) Weller, A.; Nolting, K.; Steark, H. *Chem. Phys. Lett*. **1983**, *96*, 24.

(29) Schulten, K.; Wolynes, P. G. J. *Chem. Phys*. **1978**, *68*, 3292.

(30) Hayashi, H.; Nagakura, S. *Bull. Chem. Soc. Jpn*. **1978**, *51*, 2862.

(31) (a) Noyes, R. M. *J. Am. Chem. Soc*. **1956**, *78*, 5486. (b) Kaptein, R. *J. Am. Chem. Soc*. **1971**, *94*, 6251.

(32) (a) Noyes' reencounter function is based on the random flight theory, where the interaction potential between the particles is assumed to be zero. For more rigorous description of dynamic behaviors of RIPs with unlike charges, a numerical method such as the procedure derived by Aminov and Pedersen[32b] may be necessary. However, at a qualitative level of discussion, we use the parameters α, m, and β in relation to the rates of the processes shown in Scheme 1B. (b) Aminov, K. L.; Pedersen, J. B. *Chem. Phys*. **1995**, *193*, 297.

(33) Kaptein reported that m (∼10^{-6} s$^{1/2}$) is not very much affected by viscosity.[31b]

(34) (a) Wakasa, M.; Nishizawa, K.; Abe, H.; Kido, G.; Hayashi, H. *J. Am. Chem. Soc*. **1999**, *121*, 9191. (b) The asymptotic value of the relative yield of the escaped radical, $Y_{\Delta gM}(B \rightarrow \infty)$, depends on the initial population among the spin sublevels of ^{3}RP. When ^{3}RP is formed from a triplet precursor with a population of the Boltzman distribution, the three sublevels (T_0, $T_{\pm1}$) of ^{3}RP are almost equally populated, and the $Y_{\Delta gM}(B \rightarrow \infty)$ value is $^2/_3$.

(35) Sano, H.; Tachiya, M. *J. Chem. Phys*. **1979**, *71*, 1276.

(36) (a) Smaller separation rates (5×10^6 to 1×10^7 s^{-1}) were reported by means of time-resolved EPR techniques for geminate RIPs generated through photoinduced ET reactions in polar solvents such as EtOH and 2-PrOH.[36b,c] In the present case, however, with such a small k_{sep} value, Φ_{FI} (0 T) would be much lower and $R(B)_{max}$ would be much larger than the respective observed values. Although we have no idea accounting for such a discrepancy at present, the separation process of SSRIP to free ions may not be represented well by a single-exponential function with a rate constant of k_{sep}. (b) Matsuyama, A.; Maeda, K.; Murai, H. *J. Phys. Chem. A* **1999**, *103*, 4137. (c) van Willigen, H.; Levstein, P. R.; Ebersole, M. *Chem. Rev*. **1993**, *93*, 173.

(37) Steinfeld, J. I.; Francisco, J. S.; Hase, W. L. *Chemical Kinetics and Dynamics*; Prentice Hall Inc.: Englewood Cliffs, NJ, 1989; Chapter 4.

(38) Werner, H.-J.; Schulten, Z.; Schulten, K. *J. Chem. Phys*. **1977**, *67*, 646.

(39) Nakai, T.; Tani, M.; Nishio, S.; Matsuzaki, A.; Sato, H. *J. Phys. Chem. A* **1999**, *103*, 355.

(40) (a) Marcus, R. A. *J. Chem. Phys*. **1956**, *24*, 966. (b) Marcus, R. A. *J. Chem. Phys*. **1956**, *24*, 979.

(41) (a) Kobori, Y.; Sekiguchi, S.; Akiyama, K.; Tero-Kubota, S. *J. Phys. Chem. A* **1999**, *103*, 5416. (b) Kobori, Y.; Akiyama, K.; Tero-Kubota, S. *J. Chem. Phys*. **2000**, *113*, 465.

(42) (a) Volk, M.; Häberle, T.; Feick, R.; Ogrodnik, A.; Michael-Beyerle, M.-E. *J. Phys. Chem*. **1993**, *97*, 9831. (b) Okamura, M. Y.; Isaacson, R. A.; Feher, G. *Biochim. Biophys. Acta* **1979**, *546*, 394.

(43) Kaptein, R.; Oosterhoff, J. L. *Chem. Phys. Lett*. **1969**, *4*, 195.

(44) (a) In the reaction of ^{3}MPTZ* with PI, the multiplet (E/A) polarization due to the radical pair mechanism (RPM) was rather weak and overlapped with net emissive (E) polarization due to the triplet mechanism (TM). In the other reactions, the contribution of the TM was much smaller than that of the RPM. The weaker RPM polarization in the reaction of ^{3}MPTZ* with PI than that in the other ones suggested that the $|J|$ value of [MPTZ$^{\bullet+}$PI$^{\bullet-}$] should be smaller than that of the other SSRIPs. For backward ET reactions of SSRIPs with $|\lambda + \Delta G_{BET}|$ values close to zero, eq 9 cannot be applied and the $|J|$ values of the SSRIPs become close to zero.[41,42] From these facts, the backward ET of [MPTZ$^{\bullet+}$PI$^{\bullet-}$] is likely close to the barrierless point. (b) MFEs for the ET reaction of ^{3}MPTZ* with PI in 2-PrOH were previously reported.[44c] The $\alpha m/(1-\beta)$ value for this reaction was determined to be 1.15×10^{-5} s$^{1/2}$, which was similar to those for the reactions investigated here. (c) Mori, Y.; Sakaguchi, Y.; Hayashi, H. *J. Phys. Chem. A* **2000**, *104*, 4896.

(45) Nelsen, S. F.; Blackstock, S. C.; Kim, Y. *J. Am. Chem. Soc*. **1987**, *109*, 677.

(46) Dewar, M. S. J.; Zoebisch, E. G.; Healy, E. F.; Stewart, J. J. P. *J. Am. Chem. Soc*. **1985**, *107*, 3902.

(47) (a) Efrima, S.; Bixon, M. *Chem. Phys. Lett*. **1974**, *25*, 34. (b) Efrima, S.; Bixon, M. *Chem. Phys*. **1976**, *13*, 447. (c) Ulstrup, J. Jortner, J. *J. Chem. Phys*. **1975**, *63*, 4358. (d) Jortner, J. *J. Chem. Phys*. **1976**, *64*, 4860.

(48) Several experimental studies indicated that k_{sep} varies with not only the parameters in eq 11 but also other properties of particular D$^{\bullet+}$−A$^{\bullet-}$ pairs. See 2b, 6b, 6c.

(49) As ϵ_r increases, SSRIP is more stabilized than CRIP and k_{solv} increases. See 4d, 4e, 4g.

(50) Under the condition of $k_{BET} \gg k_{HFC}$, k_{sep}, the ϕ_{sep}(0 T) value can be approximated as $\phi_{sep}(0\ T) \approx k_{sep}/(k_{HFC}+k_{sep})$. With the observed Φ_{FI}(0 T) value ($\phi_{sep}(0\ T) \geq \Phi_{FI}(0\ T) = 0.71$) and the estimated k_{HFC} value (1×10^8 s^{-1}), k_{sep} is estimated to be 2.5×10^8 s^{-1}, which is larger than the value evaluated by eq 11 (1×10^8 s^{-1}). This discrepancy may be partially attributed to the underestimation of D by Stokes−Einstein relationship with the stick boundary condition.

(51) Petrov, N. Kh.; Borisenko, V. N.; Starostin, A. V.; Alifimov, M. V. *J. Phys. Chem*. **1992**, *96*, 2901.

(52) Föll, R. E.; Kramer, H. E. A.; Steiner, U. E. *J. Phys. Chem*. **1990**, *94*, 2476.

(53) Khudyakov, I. V.; Serebrennikov, Y. A.; Turro, N. J. *Chem. Rev*. **1993**, *93*, 537.

(54) We cannot determine whether the primary intermediates should be refer as "^{3}CRIP" or "^{3}Ex*", but use the term "^{3}CRIP" herein.

(55) It was reported for the fluorescence quenching in MeCN that the quenching distance increases with decrease in ΔG_{ET}. See 3f.

(56) (a) The ΔG_{BET} dependence of k_{BET} for CRIP is different from that for SSRIP. (b) Mataga, N.; Miyasaka, H. In *Electron Transfer: from Isolated Molecules to Biomolecules*; Bixon, M., Jortner, J., Eds.; Wiley: New York, 1999;, Part II, pp 431−496.

(57) Fujita, H.; Yamauchi, J. *J. Heterocycl. Chem*. **1980**, *17*, 1053.
(58) (a) Melhuish, W. H. *J. Phys. Chem*. **1961**, *65*, 229. (b) Eaton, D. F. *Pure Appl. Chem*. **1988**, *60*, 1055.
(59) (a) Dehalogenation reactions of radical anions of F- or Br-substituted benzonitrile and benzoate were observed in polar solvents. (b) Konovalov, V. V.; Laev, S. S.; Beregovaya, I. N.; Shchegoleva, L. N.; Shteingarts, V. D.; Tsvetkov, Y. D.; Bilkis, I. *J. Phys. Chem. A* **2000**, *104*, 352. (c) Behar, D.; Neta, P. *J. Am. Chem. Soc*. **1980**, *102*, 4798. (d) Neta, P.; Behar, D. *J. Am. Chem. Soc*. **1981**, *103*, 103. (e) Behar, D.; Neta, P. *J. Am. Chem. Soc*. **1981**, *103*, 2280. (f) Andrieux, C. P.; Blocman, C.; Dumas-Bouchiat, J.-M.; M'Halla, F.; Savéant, J.-M. *J. Am. Chem. Soc*. **1980**, *102*, 3806.
(60) *PCPro-K*, Global Analysis and Simulation Package for Windows95, Applied Photophysics Ltd., 1996.
(61) Rieger, P. H.; Bernal, I.; Reinmuth, W. H.; Frankel, G. K. *J. Am. Chem. Soc*. **1963**, *85*, 683.
(62) Frisch, M. J.; Trucks, G. W.; Schlegel, H. B.; Scuseria, G. E.; Robb, M. A.; Cheeseman, J. R.; Zakrzewski, V. G.; Montgomery, J. A. Jr.; Stratmann, R. E.; Burant, J. C.; Dapprich, S.; Millam, J. M.; Daniels, A. D.; Kudin, K. N.; Strain, M. C.; Farkas, O.; Tomasi, J.; Barone, V.; Cossi, M.; Cammi, R.; Mennucci, B.; Pomelli, C.; Adamo, C.; Clifford, S.; Ochterski, J.; Petersson, G. A.; Ayala, P. Y.; Cui, Q.; Morokuma, K.; Malick, D. K.;. Rabuck, A. D.; Raghavachari, K.; Foresman, J. B.; Cioslowski, J.; Ortiz, J. V.; Baboul, A. G.; Stefanov, B. B.; Liu, G.; Liashenko, A.; Piskorz, P.; Komaromi, I.; Gomperts, R.; Martin, R. L.; Fox, D. J.; Keith, T.; Al-Laham, M. A.; Peng, C. Y.; Nanayakkara, A.; Gonzalez, C.; Challacombe, M.; Gill, P. M. W.; Johnson, B.; Chen, W.; Wong, M. W.; Andres, J. L.; Gonzalez, C.; Head-Gordon, M.; Replogle, E. S.; Pople, J. A. *Gaussian 98*, Revision A.7; Gaussian, Inc.: Pittsburgh, PA, 1998.
(63) *Handbook of Chemistry and Physics*, 77th ed.; Lide, D. R., Ed.; CRC Press: Boca Raton, FL, 1996; pp 6−151.